Proceedings of the 14th European Inter-Regional Conference on Ceramics

University of Stuttgart, Germany
8th – 10th September 2014

CIEC 14
Conference Proceedings

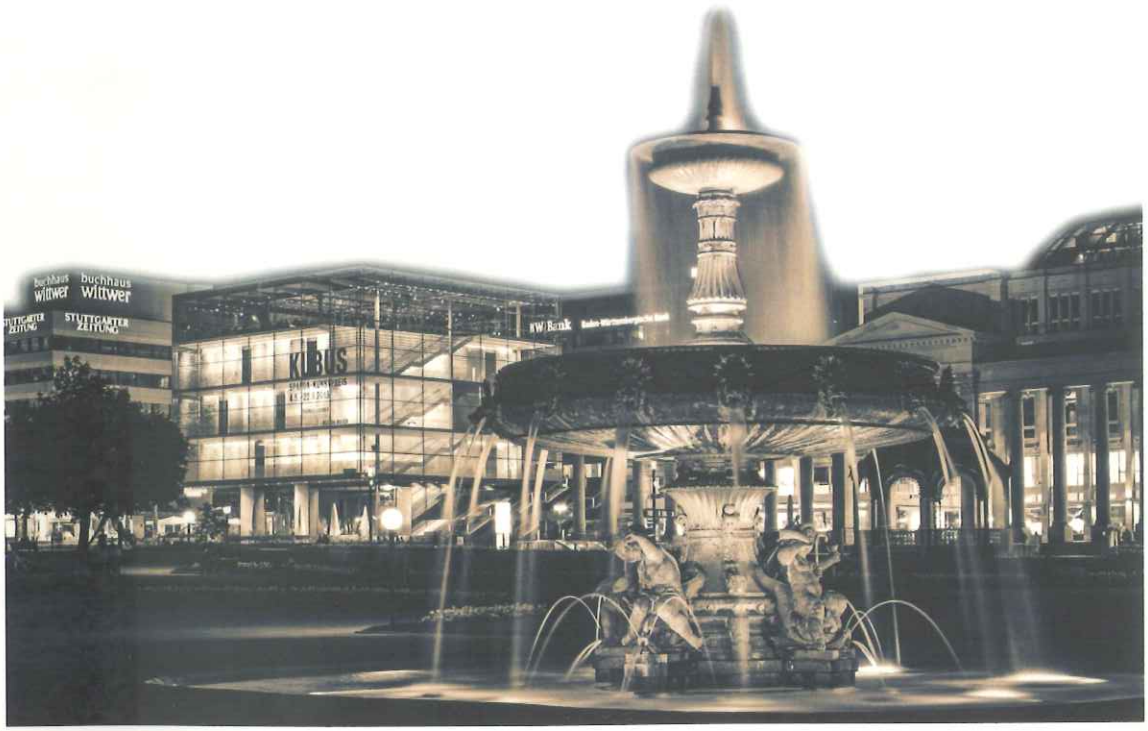

CIEC 14 Conference Proceedings
Rainer Gadow, Frank Kern (Eds.)

Micro-compression of 3Y-TZP degraded layer

Erik Camposilvan[1] and Marc Anglada[1]

[1] *Department of Materials Science and Metallurgical Engineering, Universitat Politècnica de Catalunya, Av. Diagonal 647, 08028 Barcelona – Spain*

Abstract

In the field of dental structural bioceramics, Tetragonal Polycrystalline Zirconia ceramics play an important role due to high mechanical properties, good aesthetics, low wear rate and bio-inert behavior. In these cases, surface properties are determinant especially when it comes to osseointegration or contact loading, where any deterioration is detrimental for the life of the implant. Much inquietude emerged among implants producers after finding that the surface of tetragonal zirconia undergoes a spontaneous aging phenomenon when exposed to humid environment. Many authors characterized the so called Low Temperature Degradation qualitatively, setting different techniques capable to detect and measure its progression. The degraded layer, which is normally few micrometers in depth, has been recently evaluated by means of instrumented indentation, micro-nano scratch techniques and wear tests. Nevertheless, a mechanical characterization is still missing in terms of material strength. In order to obtain this information, in this work micro-pillar compression techniques are applied, comparing the response of pillars milled directly into the degraded layer and in the non-aged material surface. Reproducible stress-strain curves were obtained and the compressive strength and elastic modulus of the degraded material could be directly compared, demonstrating that micro-compression techniques are suitable for assessing the degraded surface properties. Failure behavior appeared to be significantly different for the degraded pillars and some interesting variations could be observed when reducing the pillar diameter. All these aspects are presented and discussed in this work.

Keywords: Zirconia, micro-pillar, Low Temperature Degradation, small-scale testing.

1. Introduction

Zirconia-based ceramics represent a family of very interesting structural materials, where the tetragonal phase is conserved at room temperature in a metastable state by choosing a suitable amount of stabilizers and appropriate processing conditions, allowing the transformation toughening process to operate against crack growth. This takes place through the transformation of the metastable phase into the stable monoclinic phase, which is locally triggered by the tensile stresses arising in the vicinity of cracks during loading. The volume expansion of approximately 5% that accompanies the transformation has the key role of inducing a compressive component at the crack tip, hindering its propagation. The result is a net increase in fracture toughness, which can be of several MPa$\sqrt{m}$ depending on the stability of the tetragonal phase, which is related to the particular alloying system and microstructure. The mechanical strength of these materials is generally very high, reaching values well above 1 GPa in certain cases. The relation between fracture toughness and strength is indeed not straightforward, since for low K_{IC} values the strength is limited by flaw size, meanwhile for values above ~8 MPa$\sqrt{m}$ the limiting factor becomes the phase transformation itself, which takes place at stress levels lower than the fracture stress [1]. Here the attention is addressed to yttria-stabilized tetragonal polycrystalline zirconia (3Y-TZP), a zirconia system with very fine microstructure composed almost entirely of tetragonal grains with size of approx. 350 nm in size. The 3 mol.% of Yttrium oxide is optimized in order to attain the highest mechanical strength among single phase zirconia-based ceramics, approx. 1200 MPa in flexure for a standard processed material, and a considerable fracture toughness of ~4,5 MPa$\sqrt{m}$.

Thanks to the mentioned properties, together with a hardness of ~13 GPa, 3Y-TZP has been widely employed since the 80´s for load bearing applications under severe conditions, especially in the biomedical field. Different companies started the production of hip implants for total hip arthroplasty with zirconia femoral since the high strength could allow a more flexible design compared to other materials *e.g.* alumina [2]. Moreover, in recent years 3Y-TZP has been used for other arthroplasties and in dental implantology for the production of dental crowns, bridges, abutments and dental posts. These latter applications have been favored by the development of CAD/CAM techniques capable for shaping such components with reliability and precision [3].

The surface state and performance is of extreme importance for all the abovementioned applications, especially when it comes to load transfer from the implant to the bone or through reciprocating sliding contact. The long-term surface stability of zirconia became an issue after the discovery of hydrothermal degradation, a phenomenon that takes place in humid environment and moderate temperatures, comprising 37 °C, and affects the surface of this material. Due to the diffusion of water species, the tetragonal-monoclinic (*t-m*) transformation starts to occur spontaneously through a nucleation-and-growth mechanism. After long exposure, grain boundary microcracks are formed within the first micrometers from the surface, where monoclinic uplifts appear producing an increase in roughness [4]. The process is also accompanied by grain pull-out, a considerable decrease in surface hardness measured by nanoindentation and the deterioration of scratch resistance (Chintapalli [5], Gaillard et al. [6] and Hvizdoš et al. [7]). There is extensive literature dedicated to the study of the kinetics, crystallography and mechanisms involved in hydrothermal degradation, based on experiments performed with diverse spectroscopic and imaging techniques on the surface of samples after artificial degradation in water vapor at the standard sterilization temperature. In this way, the degradation could be observed –and eventually measured in terms of fraction of monoclinic phase content- from its first appearance on some isolated grains [8] to the progression through the first superficial layers [9] and into the volume [10]. Even though all these aspects have been widely documented, there is still lack of knowledge of how mechanical properties are modified inside the transformed volume of zirconia. It was observed by TEM that degradation microcracks develop anisotropically, with the crack planes mainly oriented almost parallel to the free surface [11]. The spatial distribution of microcracks in the degraded volume was also measured by means of focused ion beam (FIB) tomography [12], confirming the anisotropic distribution and hence suggesting that the damage produced by degradation, and so the strength inside the degraded layer, may also depend on the orientation. In the present work, the compressive mechanical behavior of the degraded layer is studied by means of small-scale testing techniques.

Small-scale testing refers to mechanical tests performed on a very reduced volume of material. A first and well-known example of these techniques is represented by nanoindentatioin, which finds its limitation in the complex stress state surrounding the indenter tip. With the development of FIB and other high precision shaping techniques coupled with the load-displacement resolution offered by the technology of nanoindenters, new methods started to appear. By creating small volume samples with suitable geometry, the response of materials to compression, bending, torsion and tension states could be probed and, in some cases (*in situ* testing into electron microscopes), directly observed. For more details about these techniques, see Legros et al. [13]. In metallic materials, the main result of these studies is that the rule "the smaller the stronger" holds for many systems and models related to strain gradients and interaction of dislocations with free surfaces have been developed for explaining the particular behavior (Greer et al. [14] and Uchic et al. [15]).

In the case of ceramics, only few authors have attempted small-scale testing approaches, employing mostly micro-pillar compression techniques with the main objective of observing the existence of a brittle-ductile transition. This can be appreciated when the sample size is reduced below some critical value that lies roughly between tens and hundreds of nanometers. In this way,

conventionally "brittle" materials have shown plasticity features at the small scale: Si [16], GaAs [17], MgO [18], alumina [19] and SiC [20]. At the same time, superelastic and shape-memory behaviors were recently observed by Lai et al. [21] during compression of zirconia micro-pillars doped with Y and Ce. Size-dependent phenomena related to flow stress in ceramic micro-pillars have also been documented by Korte and Clegg [18], showing a similar behavior to metals once dislocation activity is activated by the small size and high stresses applied.

The micro-pillar compression technique is applied also in the present study. Micro-pillars are extracted by focused ion beam from the surface of fully degraded and non-degraded 3Y-TZP, with the main target of studying the effect of degradation on the mechanical behavior.

2. Experimental

Commercial spray-dried zirconia powder (TZ-3YSB-E, Tosoh Corp.) was pressed isostatically at 200 MPa in a rod shape and sintered at 1450 °C in air inside a tubular furnace mod. Hobersal ST-18 for 2 hours, obtaining a dense ceramic with density of 6.06 ± 0.02 g/cm^3 (99.5 ± 0.3% of the theoretical value) as measured by the Archimedes' method. The rod was cut into disks of approx. 1.5 mm thickness and these were ground and polished with diamond pastes down to less than 20 nm Ra. Few samples were exposed to artificial degradation in autoclave, under steam atmosphere at 134 °C and 2 bar pressure, for 145 hours. This time was chosen in order to obtain a superficial fully degraded layer with a thickness greater than 13 μm, according to studies formerly performed on the same type of material by Muñoz Tabares and Anglada [10]. In this way, micro-sized samples could later be obtained entirely from the degraded volume. Both degraded and reference disks were then cut along the diameter and the cross-section was polished using diamond films on a tripod fixture (Struers A/S). The disk halves were mounted on inclinable holders for scanning electron microscopy (SEM) using high strength silver adhesive and coated with a few nanometers layer of Au/Pd layer to increase conductivity and avoid charging phenomena during milling.

The holders were introduced in a Zeiss Neon 40 dual beam microscope equipped with a Gemini electron column and a FIB column from Orsay Physics. The objective was to obtain by FIB milling micro-pillars with aspect ratio between 2:1 and 3:1 and different sizes, from the surface area adjacent to the cross-section edge of degraded and non-degraded disks. A major issue in this procedure is represented by the taper angle which forms when employing FIB to mill cross-sectional superficies. A way to limit this effect is to obtain the final shape with multiple steps, so that the last current can be small enough to allow careful focusing and stigmation. At the same time, the dwell time assigned to every pixel can be varied in order to optimize the milling time and the shape of the feature. The procedure was therefore optimized and micro-pillars were milled in two steps: in the first a large well, 34 μm in diameter, was obtained with a considerable ion current. In the second step, lower currents were employed and the milling profile was tuned for each pillar size. In this way, micro-pillars of 3.3 μm, 0.65 μm and 0.30 μm in diameter and reduced taper angle were obtained.

After milling, a thin cyanoacrylate strip was deposited on the surface of samples close to the milling area and the SEM holder was mounted on the stage of a MTS XP nanoindenter equipped with a CSM module for testing. Compression tests were performed with a flat-punch diamond tip machined via FIB from a Berkovich indenter. The flat surface had an equilateral triangle shape with a side of 18 μm. In order to clean the tip and align the surface of the sample, several indentations were performed on the cyanoacrylate strip and the SEM holder was tilted until a clear, symmetrical shape could be seen with the optical microscope of the nanoindenter. During a compression test, the pillar well is first imaged with the microscope and, once the target location is selected, the sample stage moves under the indenter tip. A microscope-to-indenter calibration had to be performed

each test in order to load the desired pillar with the centre of the flat surface. The uncertainty x-y stage is of 1-4 μm, so the size of the well and the indenter surfaces accounted of that.

ompression routine was designed so that thermal drift was measured in contact with the pillar beginning of the test. Afterward, loading was carried out so that the displacement rate was ximately constant, until failure of the pillar. Micro-pillars were imaged by SEM after testing.

g processing of load-displacement data, the displacement at every load value was recalculated btracting the correspondent thermal drift. Successively, the data were converted into stress- curves by taking into account the pillar height and diameter after careful measuring on SEM es. This stress is the one appearing in the upper part of the pillar, where the diameter is y smaller, that is, the maximum stress in the sample.

sults

1, the stress-strain curves of degraded (Deg) pillars of different sizes are plotted together e curve for the reference material (where AS stands for as-sintered). For the latter, only one ntative size (0.65 μm) is plotted. One curve per size is presented since the behavior was similar when repeating the test with same conditions. This is not true for very small degraded (300 nm), where significant variability in terms of failure stress and strain was recorded individual tests. In this case, two curves are presented to show the different behavior. On the lot, the theoretical elastic modulus of polycrystalline zirconia (210 GPa) is showed.

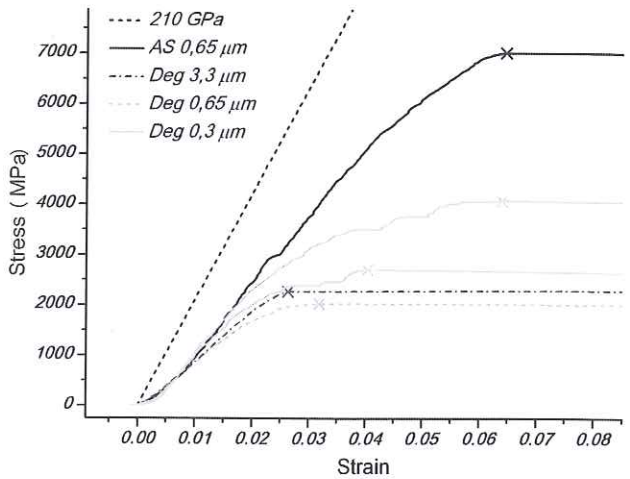

. Stress-strain curves for degraded and non-degraded micro-pillars of various diameters. indicate pillar failure. The ideal elastic modulus of tetragonal polycrystalline zirconia is ted.

SEM images of degraded pillars before and after testing are presented to appreciate the aspect.

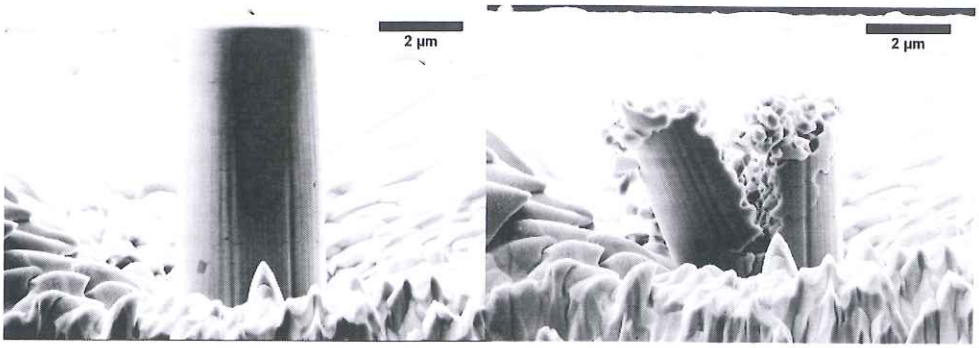

Fig. 1: Degraded 3.3 µm micro-pillar before and after compression. The intergranular character of fracture can be appreciated on the right picture.

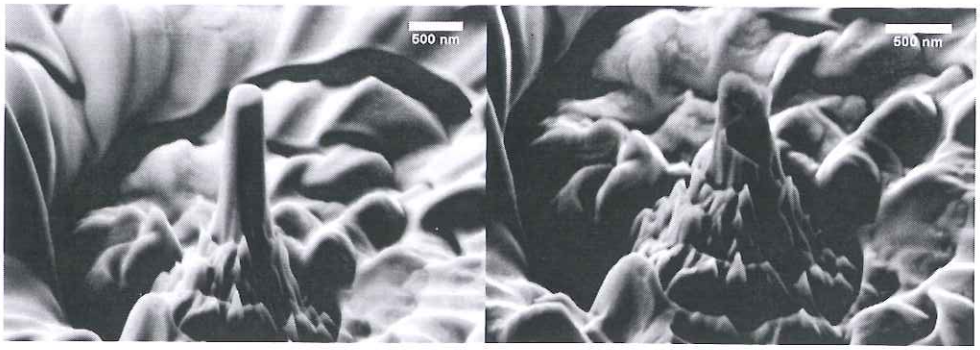

Fig. 2: Degraded 300 nm micro-pillar before and after compression. Grain pull-out during testing is evident in the picture on the right.

4. Discussion

The compressive strength of non degraded micro-pillars is of about 7 GPa, values that are significantly higher than for bulk samples, where compressive strength can be estimated around 3 GPa for 3Y-TZP processed in the same conditions. The slope of the curve initially agree with the bulk elastic modulus of polycrystalline zirconia, whereas after approximately 3 GPa a progressive deviation towards lower values is recorded, obtaining failure strains of approximately 6.5 %. These strains are considerably high for brittle ceramics, and are luckily permitted by transformation-induced plasticity. The *t-m* transformation is activated at stresses higher than 3 GPa in individual grains, and the considerable local shear strain associated with the transformation (~ 16%) is capable for accommodating the total compressive strain.

The compressive strength is markedly reduced after degradation, rounding the 2000 MPa for the 3.3 µm and 0.65 µm pillars. In these cases, the presence of degradation microcracks, which can be already observed before testing on the left side of Fig. 2, affects strongly the mechanical response of the micro-pillars. Since these microcracks are mainly distributed along planes approximately parallel to the surface of the sample, the initial stiffness is only slightly reduced. As long as the load increase during testing, microcracks can grow along the weakened grain boundaries until failure occurs by axial splitting of the pillar. The final fracture is completely intergranular with the presence of debris as it can be observed on the right side of Fig. 2.

In the case of the smallest degraded pillars, the behavior significantly differs from one test to another. Since the grain size of this material is of 350 nm, one can imagine that inside a pillar that is ~ 300 nm in diameter and ~ 900 nm in height, only few grains and related grain boundaries are present. This is reflected on the initial slope of the stress-strain curves, which is steeper than for bigger pillars, and on the failure stress and strains, which values are generally higher and can reach sometimes the ones recorded for non-degraded samples. In these cases, a series of strain events can be appreciated on the curves, which can be reasonably related to crack growth along grain boundaries or sliding of already cracked interfaces under high compressive stress. The fracture is still completely intergranular, with evidence of grain pull-out that can be observed on the right side of Fig. 3. There seems to be a general trend in terms of failure strain in relation with the pillar size for the degraded material, obtaining higher failure strains for smaller samples. At the same time, the deviation from linearity in the stress/strain curve is more pronounced when the size is reduced thanks to the contribution of local crack growth and opening or sliding of crack surfaces.

5. Conclusions

Micro-compression experiments have been performed on micro-pillars milled by FIB from the zirconia superficial degraded layer. The compressive failure strength and strain are reduced by at least a factor of 3 and 2 after degradation, respectively, due to the presence of degradation microcracks. In compression, the microcracks only slightly affect the initial stiffness of micro-pillars, meanwhile the effect is more pronounced when the load is increased. Reducing the pillar size in the nanometer range results in a variable response justified by the contribution of individual degradation microcracks to the stress-strain curve.

Reference list

1. Hannink, R. H. J.; Kelly, P. M.; and Muddle, B. C.: Transformation Toughening in ZrO2-Containing Ceramics, *J. Am. Ceram. Soc.*, Vol. **83**, No. 3, 2000, pp. 461–487.
2. Chevalier, J.; Gremillard, L.; and Deville, S.: Low-Temperature Degradation of Zirconia and Implications for Biomedical Implants, *Annu. Rev. Mater. Res.*, Vol. **37**, No. 1, 2007, pp. 1–32.
3. Miyazaki, T.; Hotta, Y.; Kunii, J.; Kuriyama, S.; and Tamaki, Y.: A review of dental CAD/CAM: current status and future perspectives from 20 years of experience., *Dent. Mater. J.*, Vol. **28**, No. 1, 2009, pp. 44–56.
4. Lawson, S.: Environmental Degradation of Zirconia Ceramics, *J. Eur. Ceram. Soc.*, Vol. **15**, 1995, pp. 485–502.
5. Chintapalli, R. K.: Influence of sandblasting on zirconia in restorative dentistry, Universitat Politécnica de Catalunya, 2012.
6. Gaillard, Y.; Jiménez-Piqué, E.; Soldera, F.; Mücklich, F.; and Anglada, M.: Quantification of hydrothermal degradation in zirconia by nanoindentation, *Acta Mater.*, Vol. **56**, No. 16, 2008, pp. 4206–4216.
7. Hvizdoš, P.; Chintapalli, R. K.; Valle, J.; and Anglada, M.: Effect of Low Temperature Degradation on Scratch Behaviour of 3Y-TZP, *Key Eng. Mater.*, Vol. **413**, 2009, pp. 322–325.
8. Tsubakino, H.; Kuroda, Y.; and Niibe, M.: Surface Relief Associated with Isothermal Martensite in Zirconia-3-mol%-Yttria Ceramics Observed by Atomic Force Microscopy, *J. Am. Ceram. Soc.*, Vol. **82**, No. 10, 1999, pp. 2921–2923.
9. Garvie, R. C. and Nicholson, P. S.: Phase analysis in zirconia systems, *J. Am. Ceram. Soc.*, Vol. **55**, No. 6, 1972, pp. 303–305.

10. Muñoz Tabares, J. A. and Anglada, M.: Quantitative Analysis of Monoclinic Phase in 3Y-TZP by Raman Spectroscopy, *J. Am. Ceram. Soc.*, Vol. **93**, No. 6, 2010, pp. 1790–1795.

11. Muñoz Tabares, J. A.; Jiménez-Piqué, E.; and Anglada, M.: Subsurface evaluation of hydrothermal degradation of zirconia, *Acta Mater.*, Vol. **59**, No. 2, 2011, pp. 473–484.

12. Jiménez-Piqué, E.; Ramos, A.; Muñoz Tabares, J. A.; Hatton, A.; Soldera, F.; Mücklich, F.; and Anglada, M.: Focused ion beam tomography of zirconia degraded under hydrothermal conditions, *J. Eur. Ceram. Soc.*, Vol. **32**, No. 10, 2012, pp. 2129–2136.

13. Legros, M.; Gianola, D. S.; and Motz, C.: Quantitative In Situ Mechanical Testing in Electron Microscopes, *Mater. Res. Soc. Bull.*, Vol. **35**, 2010, pp. 354–360.

14. Greer, J. R. and De Hosson, J. T. M.: Plasticity in small-sized metallic systems: Intrinsic versus extrinsic size effect, *Prog. Mater. Sci.*, Vol. **56**, No. 6, 2011, pp. 654–724.

15. Uchic, M. D.; Dimiduk, D. M.; Florando, J. N.; and Nix, W. D.: Sample dimensions influence strength and crystal plasticity., *Science*, Vol. **305**, No. 5686, 2004, pp. 986–9.

16. Östlund, F.; Rzepiejewska-Malyska, K.; Leifer, K.; Hale, L. M.; Tang, Y.; Ballarini, R.; Gerberich, W. W.; and Michler, J.: Brittle-to-Ductile Transition in Uniaxial Compression of Silicon Pillars at Room Temperature, *Adv. Funct. Mater.*, Vol. **19**, No. 15, 2009, pp. 2439–2444.

17. Michler, J.; Wasmer, K.; Meier, S.; Östlund, F.; and Leifer, K.: Plastic deformation of gallium arsenide micropillars under uniaxial compression at room temperature, *Appl. Phys. Lett.*, Vol. **90**, 2007.

18. Korte, S. and Clegg, W. J.: Discussion of the dependence of the effect of size on the yield stress in hard materials studied by microcompression of MgO, *Philos. Mag.*, Vol. **91**, No. 7–9, 2011, pp. 1150–1162.

19. Montagne, A.; Pathak, S.; Maeder, X.; and Michler, J.: Plasticity and fracture of sapphire at room temperature : Load-controlled microcompression of four different orientations, *Ceram. Int.*, 2013, pp. 1–8.

20. Zhang, Y.; Han, X.; Zheng, K.; Zhang, Z.; Zhang, X.; Fu, J.; Ji, Y.; Hao, Y.; Guo, X.; and Wang, Z. L.: Direct Observation of Super-Plasticity of Beta-SiC Nanowires at Low Temperature, *Adv. Funct. Mater.*, Vol. **17**, No. 17, 2007, pp. 3435–3440.

21. Lai, A.; Du, Z.; Gan, C. L.; and Schuh, C. a: Shape memory and superelastic ceramics at small scales., *Science*, Vol. **341**, No. 6153, 2013, pp. 1505–8.